

Static contact angle algorithm selection for superhydrophobic surface hydrophobicity detection

Zhiniu Xu

Hebei Provincial Key Laboratory of Power Transmission Equipment Security Defense, North China Electric Power University, Baoding 071003, People's Republic of China
E-mail: wzcjxx@163.com

Published in Micro & Nano Letters; Received on 11th August 2013; Revised on 4th November 2013; Accepted on 22nd November 2013

The static contact angle calculation for superhydrophobic surfaces is systematically investigated. The water drop profiles with different volumes, contact angles, rotational angles and apex coordinates are numerically generated based on the Laplace equation. Thereafter, the goniometry, $\theta/2$ method, circle and ellipse fitting algorithms and an improved axisymmetric drop shape analysis-profile (ADSA-P) algorithm are used to calculate the static contact angle. The results reveal that the contact angle errors by the $\theta/2$ method, circle and ellipse fitting algorithms increase with the drop volume/contact angle. The goniometry will introduce significant error. The ADSA-P algorithm can accurately obtain the contact angles (error $< 0.3^\circ$) for the drop profiles regardless of the water drop volume, contact angle, rotational angle and apex coordinate. The ADSA-P algorithm should be selected to calculate the static contact angles for the superhydrophobic surfaces. Static contact angle measurements of the superhydrophobic surfaces validate the aforementioned analysis.

1. Introduction: Surfaces with water contact angles larger than 150° and sliding angles smaller than 10° are generally classified as superhydrophobic surfaces [1]. Superhydrophobic surfaces have experienced extensive exploration [2]. For material with a flat surface, the water contact angle of the material is not more than 120° [3], even when coated with a monolayer of perfectly close-hexagonal-packed- CF_3 groups. Therefore, hydrophobic surfaces, and micro and nanostructures [4, 5] are generally required to realise superhydrophobic surfaces. Wettability is crucial for superhydrophobic surfaces and it is directly characterised by the static contact angle [5, 6].

Owing to ease of use, goniometry [6] is often used to calculate the contact angle. On the basis of the approximate or exact models, the $\theta/2$ method (height-width method) [7], the circle [8] and the ellipse fitting algorithms [9, 10], the axisymmetric drop shape analysis-profile (ADSA-P) algorithm is proposed [11–13] and is prevalent in static contact angle calculation. The ADSA-P algorithm has relatively high accuracy for the drop images with large contact angles. However, the algorithm is more complex and time-consuming. The other four algorithms are relatively simple and efficient to compute and sometimes they may actually be preferable to calculate the contact angle. Whether the ADSA-P algorithm can be replaced by the aforementioned four simple algorithms is still unknown. To sum up, the contact angle algorithm selection for superhydrophobic surfaces must be studied.

In this Letter, an improved ADSA-P algorithm [11], the goniometry [14], the $\theta/2$ method [7], the circle and the ellipse fitting algorithms [8, 9] are implemented. The accuracies and the applicability of the aforementioned five algorithms are analysed and the selection rule of the contact angle algorithm for superhydrophobic surfaces is given. The results are validated by the static contact angle measurements of the real water drop images of the superhydrophobic surfaces.

2. Validation of the Laplace equation

2.1. Laplace equation: Generally, in static contact angle measurement, the surfaces, even the superhydrophobic surfaces, are considered to be the homogeneous surface [9, 11, 15]. Fig. 1 represents the meridian profile of an axisymmetric sessile drop resting on a horizontal surface.

The profile can be written as the following system of ordinary differential equations [11]

$$\begin{cases} \frac{dx}{ds} = \cos \theta \\ \frac{dz}{ds} = \sin \theta \\ \frac{d\theta}{ds} = 2b + cz - \sin \theta/x \end{cases} \quad (1)$$

where s is the arc length measured from the origin, $c = g\Delta\rho/\gamma$ is the capillary constant of the system and b is the curvature at the origin of the coordinates, θ is the tangential angle as shown in Fig. 1, $\Delta\rho$ is the difference in the densities of the two bulk phases, g is the gravitational acceleration and γ is the interfacial tension.

2.2. Validation of the Laplace equation: The Laplace equation has been extensively used in the analysis of the static contact angle algorithm [8, 9, 16]. However, its validity has not been systematically analysed. To validate further the Laplace equation, the following analysis is given. The water drop image with a drop volume of $40 \mu\text{l}$ is acquired by a SL200B contact angle measuring instrument, and the surface is the room temperature vulcanised silicone rubber coating which is covered with a pollution layer [9]. The fitted and the calculated results for the image are shown in Fig. 2.

As shown in Fig. 2, the profile obtained by the ADSA-P algorithm gives good agreement with the experimental water drop profile. The calculated contact angle 151.86° is an accurate value.

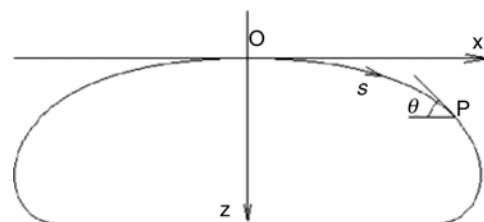


Figure 1 Coordinates system for axisymmetric liquid–fluid interfaces

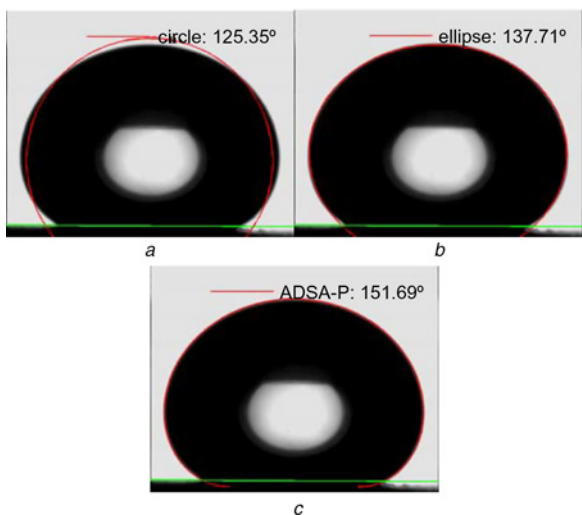


Figure 2 Calculated results of the real water drop image of the superhydrophobic surface by the three algorithms
 a Circle fitting algorithm
 b Ellipse fitting algorithm
 c ADSA-P algorithm

The $\theta/2$ method gives a contact angle of 126.23° . If the contact angle given by the ADSA-P algorithm is considered to be the correct value, then the errors of the $\theta/2$ method and the circle and the ellipse fitting algorithms are -25.46° , -26.34° and -13.98° , respectively.

To validate the Laplace equation, a water drop profile with a volume of $39.66 \mu\text{l}$ and a contact angle of 152.17° (similar to the real water drop image) is numerically generated based on (1). The obtained edges of the circle and the ellipse fitting algorithms, and the ADSA-P algorithm for the aforementioned numerically generated profile are illustrated in Fig. 3. The contact angles calculated by the $\theta/2$ method, the circle and the ellipse fitting algorithms and the ADSA-P algorithm are 126.17° , 123.59° , 137.60° and 152.17° , respectively, and the errors are -25.99° , -28.58° , -14.57° and 0.02° , respectively.

From the comparison of Figs. 2 and 3, it can be seen that not only the calculated contact angles but also the edges in Fig. 3 agree well

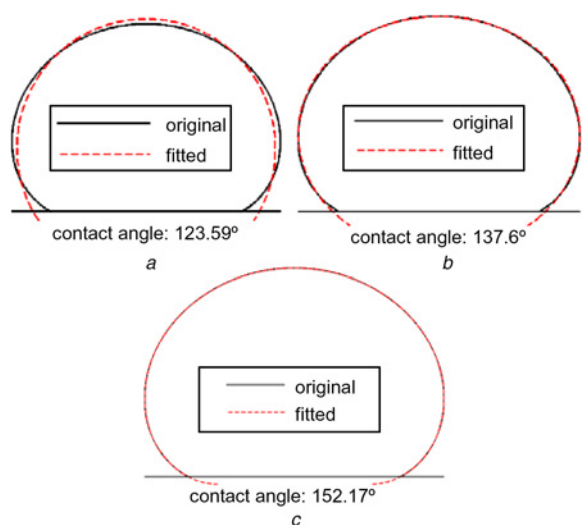


Figure 3 Calculated results of a numerically generated water drop profile similar to the real water drop image by the three algorithms
 a Circle fitting algorithm
 b Ellipse fitting algorithm
 c ADSA-P algorithm

with that of the real water drop image in Fig. 2. As a result, the Laplace equation is well validated by the aforementioned results. Therefore the analysis in Sections 3 and 4 is reliable.

3. Comparison of different algorithms: Two water drop profiles with a rotational angle [11] of 2° are numerically generated and the contact angles are 165.08° and 165.19° , respectively, and the drop volumes are 1.12 and $104.79 \mu\text{l}$, respectively. Apart from the $\theta/2$ method, the calculated and the fitted results by the other algorithms are displayed in Figs. 4 and 5, respectively.

As shown in Fig. 4, the errors are -4.21° , -6.48° , -5.31° and 0.23° , respectively. The goniometry is performed ten times, and the mean value and the standard deviation of the errors are -5.26° and 0.92° , respectively. The calculated contact angle and the error by the $\theta/2$ method are 158.84° and -6.24° , respectively. From Fig. 5, it can be seen that the errors are -8.75° , -50.68° , -25.28° and 0.14° , respectively. The mean value and the standard deviation of the errors of the goniometry are -10.12° and 1.58° , respectively. The contact angle result and the error by the $\theta/2$ method are 119.50° and -45.69° , respectively.

Obviously, apart from the ADSA-P algorithm, the other algorithms will give rise to significant errors when they are used to calculate the static contact angle for the superhydrophobic surfaces. The accuracy of the ADSA-P algorithm is high and the maximum error is 0.23° only, and at the same time, the calculated edges coincide with the experimental profiles, which also validates the algorithm.

For the above two profiles, the goniometry introduces significant errors. However, the calculated results are relatively stable. Generally, the results may be considered as the accurate values by the operators and thus the significant error will be neglected. For Figs. 4b, c and 5c (the circle and the ellipse fitting algorithms are used), the whole or a large fraction of the obtained edges coincide with that of the desired ones. However, the contact angle errors are -6.48° , -5.31° and -25.28° , respectively. The results may be considered as accurate ones by the operator even if the fitted edges are shown. Therefore the significant error may also be neglected.

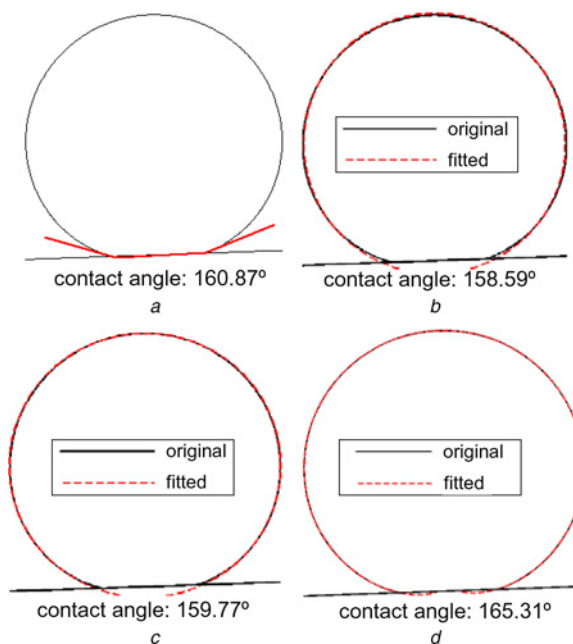


Figure 4 Calculated results of a water drop profile with a volume of $1.12 \mu\text{l}$ and a contact angle of 165.08° by the four algorithms
 a Goniometry
 b Circle fitting algorithm
 c Ellipse fitting algorithm
 d ADSA-P algorithm

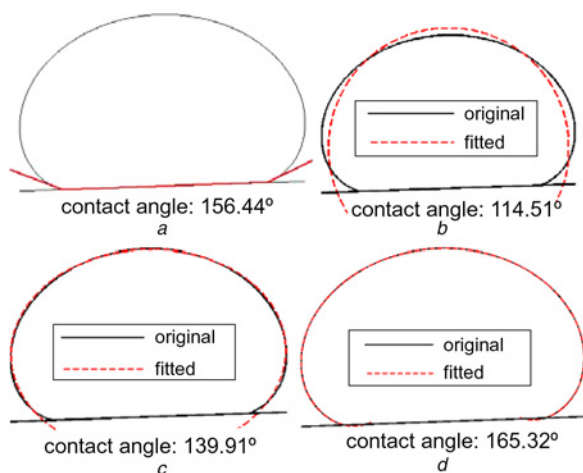


Figure 5 Calculated results of a water drop profile with a volume of 104.79 μl and a contact angle of 165.19° by the four algorithms
 a Goniometry
 b Circle fitting algorithm
 c Ellipse fitting algorithm
 d ADSA-P algorithm

The aforementioned cases reveal that algorithm selection is vital for the static contact angle measurements for the superhydrophobic surfaces. If the inappropriate algorithm is selected, then the large errors may be introduced by the algorithm and more importantly, the operator may not recognise it. However, the improved ADSA-P algorithm has high accuracy, and it can effectively handle the drops with different parameters and avoid the aforementioned issues.

4. Analysis of the influencing factors: The goniometry has relatively low accuracy and high workload, and there are so many water drop profiles that need to be processed in this Section. Therefore goniometry is not used to calculate the static contact angles.

4.1. Water drop volume: In the static contact angle measurements for the superhydrophobic surfaces, the water drop volumes can be selected as about 2 μl [2], 3 μl [4], about 4 μl [5], 5 μl [1, 3], 20 μl [17], respectively. Without loss of generality the contact angle is set to about 165°. At the same time, on consideration of slightly unrealistic or excessive volume, the range of the water drop volume is in the interval of 1–50 μl . The contact angle errors of the four algorithms with different water drop volumes are shown diagrammatically in Fig. 6.

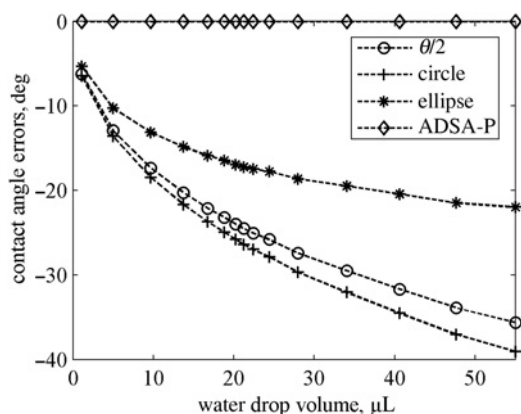


Figure 6 Change of the contact angle errors of the four algorithms with the water drop volume

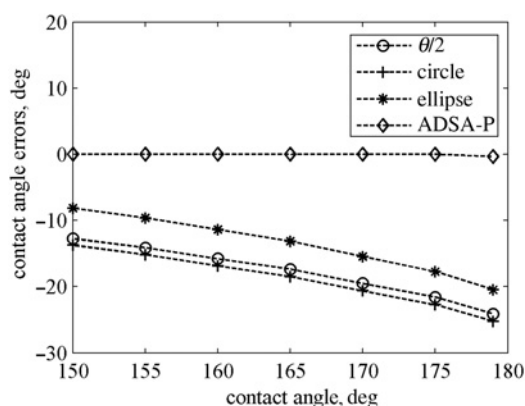


Figure 7 Change of the contact angle errors of the four algorithms with the contact angle

As can be seen from Fig. 6, the contact angle errors of the $\theta/2$ method, and the circle and the ellipse fitting algorithms increase with the water drop volume. The three algorithms introduce significant errors and the maximum errors are -35.6° , -39.1° and -22.0° , respectively, when the water drop volume reaches 54.98 μl . However, as the ADSA-P algorithm is developed on the basis of the Laplace equation, it has high accuracy and the maximum error is -1.50×10^{-3} only.

4.2. Contact angle: The contact angles of the superhydrophobic surfaces are greater than 150° and may reach about 180° [2]. Without loss of generality, the water drop volume is selected as about 10 μl , and the range of the contact angle is in the interval of 150°–179°. The contact angle errors are displayed in Fig. 7.

As can be seen from Fig. 7, the contact angle errors of the $\theta/2$ method, and the circle and the ellipse fitting algorithms increase with the contact angle and the maximum errors are -24.11° , -25.28° and -20.48° , respectively, when the real contact angle reaches 179°. However, the ADSA-P algorithm has high accuracy with the contact angle from 150° up to 179°, and the maximum error is -0.16° only.

4.3. Rotational angle: Without loss of generality, the water drop volume and the contact angle are selected as 9.68 μl and 164.77°, respectively, and the rotational angle [11] is in the interval of -2° and 2° . The contact angle errors are demonstrated in Fig. 8.

It can be seen in Fig. 8 that the errors of the four algorithms are -17.42° , -18.53° , -13.13° and 0.19° , respectively, and remain nearly constant with the increasing of the rotational angle. Similar

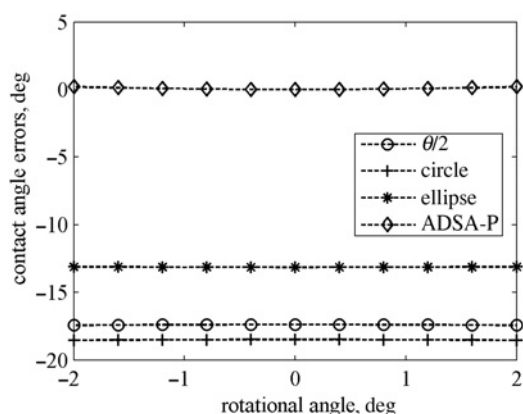


Figure 8 Change of the contact angle errors of the four algorithms with the rotational angle

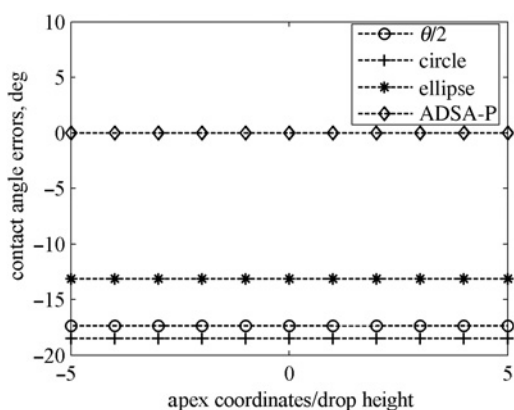


Figure 9 Change of the contact angle errors of the four algorithms with the apex coordinates

to Figs. 6 and 7, the ADSA-P algorithm has high accuracy with different rotational angles.

4.4. Apex coordinates: Without loss of generality, the water drop volume is selected as $9.68 \mu\text{l}$, the contact angle is 164.77° and the x and y coordinates of the apex are in the interval of -5 and 5 times of the drop height. The contact angle errors are illustrated in Fig. 9.

From Fig. 9, we discover that the errors of the four algorithms are -17.37° , -18.48° , -13.13° and -8.49×10^{-4} , respectively, and remain constant with the increasing of the apex coordinates. Similar to Figs. 6 to 8, the ADSA-P algorithm has high accuracy with different apex coordinates.

4.5. Discussion: To sum up, the contact angle errors of the other algorithms increase with the water drop volume and the contact angle. Thus, the small volume's and the contact angle's water drops will correspond to relatively small errors. A water drop profile with a volume of $1.10 \mu\text{l}$ and a contact angle of 150.06° is numerically generated and used to evaluate the accuracy and the applicability of the aforementioned three algorithms. The errors are -3.83° , -4.07° and -2.74° , respectively. Generally, the static contact angles of the superhydrophobic surfaces are higher than 150° [1], even close to 180° [2] and then even if the water drop volume is selected as $1 \mu\text{l}$, the errors of the aforementioned three algorithms are large. At the same time, a too small water drop volume will cause difficulty in the conduction of the static contact angle measurement. If the real contact angle is equal to 150° , the critical water drop volumes of the aforementioned three algorithms corresponding to contact angle errors of 1° , 2° and 3° , expressed by V_1 , V_2 and V_3 , respectively, are listed in Table 1.

The critical water drop volumes in Table 1 may be too small to operate in the static contact angle experiments. However, the accuracy of the ADSA-P algorithm in different contact angles and water drop volumes is high and the maximum error is only 0.23° . As a consequence, in conjunction with the analysis in Sections 3 and 4, not the goniometry, the $\theta/2$ method, or the circle and the

Table 1 Critical water drop volumes corresponding to the contact angle errors of 1° (V_1), 2° (V_2) or 3° (V_3) and the real contact angle of 150°

Algorithm	$V_1, \mu\text{l}$	$V_2, \mu\text{l}$	$V_3, \mu\text{l}$
$\theta/2$	0.16	0.42	0.77
circle	0.13	0.37	0.70
ellipse	0.22	0.70	1.33

ellipse fitting algorithms but the ADSA-P algorithm should be selected to calculate the static contact angles for the superhydrophobic surfaces.

5. Experimental validation: An image of the water drop dropped onto the superhydrophobic surfaces is acquired. The water drop volume is approximately $9 \mu\text{l}$, and the sample is the aluminium surface with a micro/nanostructure [18]. The principal objective of the current Letter is to decrease the error caused by the algorithm selection. To avoid the interferences caused by the seeing of the contact line, in this Letter, it is detected manually. All the five algorithms are used to calculate the static contact angles. Apart from the $\theta/2$ method, the fitted and the calculated results of the other algorithms are plotted in Fig. 10.

As seen in Fig. 10, the profile obtained by the ADSA-P algorithm gives good agreement with the experimental water drop profile. This consists of the results in Section 3, and the contact angle calculated by the algorithm, 166.15° is an accurate value. The $\theta/2$ method gives a contact angle of 148.16° and the errors of the goniometry, the $\theta/2$ method and the circle and the ellipse fitting algorithms are -14.26° , -17.99° , -18.44° and -13.44° , respectively. Similar to the results in Sections 3 and 4, the aforementioned four algorithms will introduce significant errors.

The fitted edge obtained by the circle fitting algorithm is inconsistent with the experimental profile, which consists of the results in Section 3. Apart from the contact points of the water drop, the fitted edge obtained by the ellipse fitting algorithm agrees well with the experimental profile. The difference may not be recognised by the operator, and the result may be considered to be an accurate one.

The mean value and the standard deviation of the contact angle according to ten times of calculation by the goniometry are 152.18° and 1.14° , respectively. The error of the goniometry is -13.97° . The results coincide with the results in Section 3, that is, the contact angles calculated by the goniometry have significant error. However, the calculated results are relatively stable. Therefore the results may be considered as the accurate values by the operators and thus the significant error will be neglected.

To further confirm the validity of the aforementioned analysis, a water drop profile with a volume of $8.99 \mu\text{l}$ and a contact angle of 166.36° (similar to the first real water drop image) is numerically

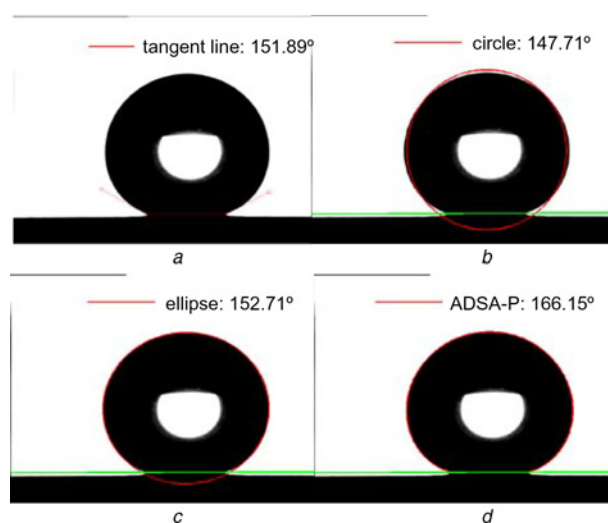


Figure 10 Calculated results of the real water drop image of the superhydrophobic surface by the four algorithms

- a Goniometry
- b Circle fitting algorithm
- c Ellipse fitting algorithm
- d ADSA-P algorithm

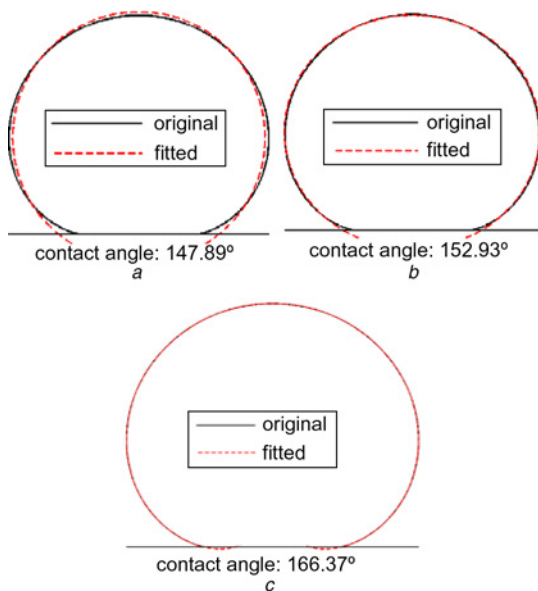


Figure 11 Calculated results of a numerically generated water drop profile similar to the real water drop image by the three algorithms

- a Circle fitting algorithm
 b Ellipse fitting algorithm
 c ADSA-P algorithm

generated based on (1). The errors of the $\theta/2$ method, the circle and the ellipse fitting algorithms and the ADSA-P algorithm are -17.39° , -18.47° , -13.44° and 2.64×10^{-4} , respectively. The obtained edges of the latter three algorithms for the numerically generated profile are illustrated in Fig. 11.

Similar to Fig. 10, the difference between the fitted edge obtained by the ellipse fitting algorithm and the desired profile may not be recognised by the operator, and the significant error may be neglected. The above results coincide with Fig. 10 and the results in Section 3. The Laplace equation is further validated by the above results.

The mean value and the standard deviation of the contact angle according to ten times of calculation by the goniometry are 142.55° and 0.79° , respectively. The error of the goniometry is -9.31° .

The aforementioned analysis results can also be used as a reference to the static contact angle measurements for the surfaces with more than 150° contact angle.

6. Conclusion: The superhydrophobic water drop profiles with different volumes, contact angles, rotational angles and apex coordinates are numerically generated based on the Laplace equation. The goniometry, the $\theta/2$ method, the circle and the ellipse fitting algorithms and the improved ADSA-P algorithm are implemented and used to calculate the static contact angles of the generated profiles and the real water drop images of the superhydrophobic surfaces. The following conclusions can be drawn from this study:

1. The goniometry will introduce significant error. However, the calculation result shows low scatter, as such, and the large errors may be neglected by the operators.
2. The errors of the $\theta/2$ method, and the circle and the ellipse fitting algorithms increase with the water drop volume/contact angle.

3. The significant error may be introduced in the circle and the ellipse fitting algorithms. However, it is not easy to be recognised by the comparison of the fitted and the desired edges.

4. The ADSA-P algorithm should be selected to calculate the static contact angle for the superhydrophobic surfaces, and the other four algorithms are not suitable for it.

7. Acknowledgments: The work was supported by the Fundamental Research Funds for the Central Universities of China (grant no. 11MG42) and the Foundation of the Hebei Educational Committee (grant no. Z2013093).

8 References

- [1] Song J.L., Xu W.J., Lu Y., Liu X., Wei Z.F., Sun J.: 'Fabrication of superhydrophobic surfaces with hierarchical rough structures on Mg alloy substrates via chemical corrosion method', *Micro Nano Lett.*, 2012, **7**, pp. 204–207
- [2] Yuan J.K., Liu X.G., Akbulut O., *ET AL.*: 'Superwetting nanowire membranes for selective absorption', *Nat. Nanotechnol.*, 2008, **3**, pp. 332–336
- [3] Zhang G., Wang D.Y., Gu Z.Z., Möhwald H.: 'Fabrication of superhydrophobic surfaces from binary colloidal assembly', *Langmuir*, 2005, **21**, pp. 9143–9148
- [4] Wu J., Yang X., Lei W., Xia J., Wang B.: 'Superhydrophobic zinc oxide film: effect of hybrid nanostructure on hydrophobicity and wetting stability', *Micro Nano Lett.*, 2013, **8**, pp. 271–273
- [5] Momen G., Farzaneh M.: 'Simple process to fabricate a superhydrophobic coating', *Micro Nano Lett.*, 2011, **6**, pp. 405–407
- [6] Pham D.C., Na K., Piao S., Cho I.J., Jhang K.Y., Yoon E.S.: 'Wetting behavior and nanotribological properties of silicone nanopatterns combined with diamond-like carbon and perfluoropolyether films', *Nanotechnology*, 2011, **22**, pp. 5303–5316
- [7] Gubanski S.M., Vlastos A.E.: 'Wettability of naturally aged silicone and EPDM composite insulators', *IEEE Trans. Power Deliv.*, 1990, **5**, pp. 1527–1535
- [8] Xu Z.N., Lü F.C.: 'A static contact angle algorithm and its application to hydrophobicity measurement in silicone rubber corona aging test', *IEEE Trans. Electr. Insul.*, 2013, **20**, pp. 1820–1831
- [9] Xu Z.N.: 'A static contact angle algorithm for silicone rubber aging experiments', *IEEE Trans. Power Deliv.*, 2013, **28**, pp. 491–498
- [10] Tang Y., Xu X., Fang J., Liang Y., Ji H.F.: 'The growth and superhydrophobicity of a perfluorocarbon nanoneedle array on a SiO₂ surface', *IEEE Trans. Nanotechnol.*, 2006, **5**, pp. 415–419
- [11] Chen P., Kwok D.Y., Prokop R.M., del R.O.I., Susnar S.S., Neumann A.W.: 'Axisymmetric drop shape analysis (ADSA) and its applications', *Stud. Surf. Sci.*, 1998, **6**, pp. 61–138
- [12] Kalantarian A., David R., Neumann A.W.: 'Methodology for high accuracy contact angle measurement', *Langmuir*, 2009, **25**, pp. 14146–14154
- [13] Kalantarian A., David R., Chen J., Neumann A.W.: 'Simultaneous measurement of contact angle and surface tension using axisymmetric drop-shape analysis-no apex (ADSA-NA)', *Langmuir*, 2011, **27**, pp. 3485–3495
- [14] Kumagai S., Yoshimura N.: 'Hydrophobic transfer of RTV silicone rubber aged in single and multiple environmental stresses and the behavior of LMW silicone fluid', *IEEE Trans. Power Deliv.*, 2003, **18**, pp. 506–516
- [15] Hung Y.L., Chang Y.Y., Wang M.J., Lin S.Y.: 'A simple method for measuring the superhydrophobic contact angle with high accuracy', *Rev. Sci. Instrum.*, 2010, **81**, pp. 065105-1–065105-9
- [16] Bortolotti M., Brugnara M., Della Volpe C., Siboni S.: 'Numerical models for the evaluation of the contact angle from axisymmetric drop profiles: a statistical comparison', *J. Colloid Interface Sci.*, 2009, **336**, pp. 285–297
- [17] Choi S.J., Suh K.Y., Lee H.H.: 'A geometry controllable approach for the fabrication of biomimetic hierarchical structure and its superhydrophobicity with near-zero sliding angle', *Nanotechnology*, 2008, **19**, pp. 5305–5309
- [18] Wang F.C., Lv F.C., Liu Y.P., Li C.R., Lv Y.Z.: 'Ice adhesion on different microstructure superhydrophobic aluminum surfaces', *J. Adhes. Sci. Technol.*, 2013, **27**, pp. 58–67